

Catalysis Science & Technology

Accepted Manuscript



This article can be cited before page numbers have been issued, to do this please use: I. Favier, M. Toro, P. Lecante, D. Pla and M. Gomez, *Catal. Sci. Technol.*, 2018, DOI: 10.1039/C8CY00901E.



This is an Accepted Manuscript, which has been through the Royal Society of Chemistry peer review process and has been accepted for publication.

Accepted Manuscripts are published online shortly after acceptance, before technical editing, formatting and proof reading. Using this free service, authors can make their results available to the community, in citable form, before we publish the edited article. We will replace this Accepted Manuscript with the edited and formatted Advance Article as soon as it is available.

You can find more information about Accepted Manuscripts in the [author guidelines](#).

Please note that technical editing may introduce minor changes to the text and/or graphics, which may alter content. The journal's standard [Terms & Conditions](#) and the ethical guidelines, outlined in our [author and reviewer resource centre](#), still apply. In no event shall the Royal Society of Chemistry be held responsible for any errors or omissions in this Accepted Manuscript or any consequences arising from the use of any information it contains.



Catalysis Science & Technology

ARTICLE

Palladium-mediated radical homo-coupling reactions: a surface catalytic insight

Isabelle Favier,^a Marie-Lou Toro,^a Pierre Lecante,^b Daniel Pla*^a and Montserrat Gómez*^a

Received 00th January 20xx,
Accepted 00th January 20xx

DOI: 10.1039/x0xx00000x

www.rsc.org/

In this contribution, we report a palladium nanoparticle-promoted reductive homocoupling of haloaryls that proceeds efficiently to produce the corresponding bis-aryls in moderate to excellent yields using a relative low catalyst loading (1 mol %), and exhibiting broad functional group tolerance. This work sheds light on how the surface state of Pd(0) nanoparticles plays a crucial role in the reactivity of catalytic systems. Notably, the proper choice of palladium salts for the preparation of the preformed nanocatalysts was a key parameter triggering a major impact in the catalytic activity; thus, the effect of halide anions on the reactivity of the as-prepared palladium nanoparticles could be assessed, being iodide anions capable to inhibit the corresponding homo-coupling reaction manifold. The homo-coupling reaction mechanism has further been studied by means of radical trap and electron paramagnetic resonance (EPR) experiments, revealing that the reaction proceeds via radical intermediates. Taking into account these data, a plausible reaction mechanism based on single-electron transfer processes on the palladium nanoparticle surface is discussed.

Introduction

Catalysed homo-coupling reactions are the synthetic tools of choice in modern organic synthesis for the synthesis of symmetrical bis-aryls. Recent research reports from Murphy, Lei, and Jiao groups on the mechanistic investigations of aryl radical generation in “homolytic aromatic substitution” reactions,^{1, 2} evidence single-electron-transfer (SET) processes where aryl halide radical anions are involved in the generation of aryl radicals and halide anions (these reports cover transition-metal free transformations).³⁻¹⁰ However, free aryl radicals remain elusive species and even recent reports by Studer *et al.* on nitroxide-mediated homo-coupling reaction of aryl Grignard reagents suggest that this type of coupling may proceed via alternative pathways.¹¹

A number of precedents concerning the Ullmann-type homocoupling of aryl halides and triflates catalysed by transition metal complexes (Pd, Ni) have been described in the literature.¹²⁻¹⁶ Notably, *in situ* formed Pd nanoparticles from metal salts have been also described for chloro- and bromoarenes in the presence of reducing agents.^{14, 16} In recent years, continuous flow technological developments using supported Pd catalysts have been successfully applied.¹⁷ Inspired by these precedents, we hypothesised that an analogous SET process could be promoted by transition metal nanoparticles and induce the fragmentation of aryl halides.¹⁸

In particular, we sought to explore different types of Pd-based catalysts (homogenous, heterogeneous and preformed nanoparticles with defined morphology and composition) in order to gain a thorough understanding on the catalytic regimes governing this transformation. In particular, improved reactivity and selectivity trends have been achieved by nanostructured catalysts in comparison to classical ones (both molecular and extended surface catalysts) in mediating the transformation of organic molecules through a precise control of the nature of catalyst.¹⁹⁻²² Accordingly, we envisaged further mechanistic studies on the reaction mechanism of C(sp²)-C(sp²) homo-coupling; a comprehensive understanding of the active species involved is of fundamental importance towards a rational optimisation of the efficiency of such processes.

Results and discussion

We focused on the reactivity and performance study of palladium-based nanocatalysts towards the homo-coupling reaction of haloarene substrates. The intrinsic properties of metal nanoparticles, in particular their electronic properties and synergistic effects among metal atoms on the surface, can trigger particular reactivity patterns, different from reactivity patterns provided by molecular species (monometallic complexes or small clusters) or extended surfaces. With the aim of studying the effect of the metal surface on the formation of bis-aryl products, surfaces mainly modified by the presence of anions (acetate, halides), we prepared well-defined palladium(0) nanoparticles (PdXNPs) starting from Pd(II) salts (where X = OAc, Cl, Br, I) in the presence of PVP as stabiliser under hydrogen pressure, following the methodology previously described by us (Figure 1).^{23, 24} This bottom-up

^a Laboratoire Hétérochimie Fondamentale et Appliquée (LHFA), Université de Toulouse 3 – Paul Sabatier and CNRS UMR 5069, 118 route de Narbonne, 31062 Toulouse Cedex 9, France. M.G. e-mail: gomez@chimie.ups-tlse.fr; D.P. e-mail: pla@lhfa.fr

^b Centre d'Elaboration de Matériaux et d'Etudes Structurales (CEMES), CNRS UPR 8011, 29 rue J. Marvig, 31055 Toulouse, France.

† Electronic Supplementary Information (ESI) available: Experimental procedures, spectral and analytical data. See DOI: 10.1039/x0xx00000x

ARTICLE

Catalysis Science & Technology

synthetic protocol afforded small (less than *ca.* 3 nm) and well-dispersed nanoparticles for **PdOAcNPs**, **PdClNPs**, and **PdBrNPs** as proven by TEM, obtaining mainly spheres together with some anisotropic nanoparticles, most likely because anions can induce anisotropic effects on the nanoparticle growth acting as face-specific capping agents.²⁵⁻²⁷ In the case of **PdINPs**, aggregation and bigger particles were observed (Figure 1). The use of glycerol as solvent together with PVP permits an efficient dispersion of the nanoparticles, avoiding their agglomeration and consequently preserving their reactivity; in addition, the use of H₂ precludes glycerol to act as reducing agent.

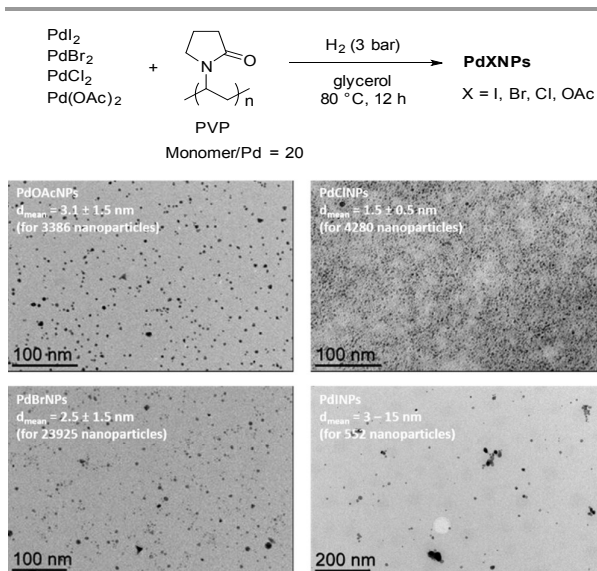


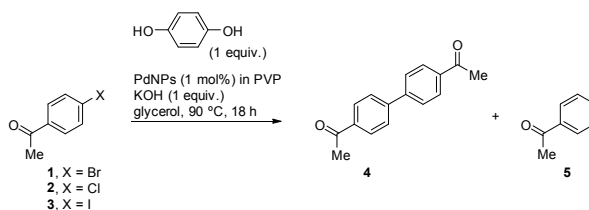
Figure 1. Synthesis of PdNPs stabilised by PVP in glycerol from Pd(II) salts and the corresponding TEM images from the corresponding glycerol colloidal solutions.

PdNPs were isolated at solid state from glycerol solutions by centrifugation. Powder X-ray diffraction analyses proved that the as-prepared nanoparticles exhibit a fcc crystalline structure (see Fig. S1 in the ESI) and the XPS analysis of **PdOAcNPs** evidenced the presence of Pd(0) and the absence of Pd(II) (see Fig. S2 in the ESI). In agreement with these data, Raman spectra of PdNPs in the region corresponding to Pd-X stretchings (400-200 cm⁻¹)^{28, 29} did not show any band, indicating that no Pd-X covalent interactions are present in these materials (see Fig. S3 in the ESI); for **PdOAcNPs**, no absorption bands were observed in the region 1700-1300 cm⁻¹, pointing that acetates are not adsorbed at the surface. However, halides can be just adsorbed at the surface, due to their high adsorption enthalpies on palladium surface.³⁰ Actually, X-ray fluorescence analyses revealed the presence of halides on the PdNPs as follows: Cl/Pd = 1/42 (2.3%), Br/Pd = 1/36 (2.7%), and I/Pd = 1/13 (7.1%), showing a significant higher amount of iodide on the nanoparticles than chlorine or bromine, according to the high affinity of iodide to palladium.³¹

The reactivity profiles using these preformed PdNPs were then investigated towards reductive carbon-carbon homo-coupling

reactions of 4'-haloacetophenones driven by hydroquinone, revealing dramatic differences triggered by the presence of the aforementioned counteranions on the reaction outcome chemoselectivity, taking into account that hydrodehalogenation is a side reaction manifold (Table 1). PdNPs prepared from Pd(OAc)₂ were more active and chemoselective (entry 1, Table 1) than those prepared from PdCl₂, PdBr₂, and PdI₂ (entries 2-4, Table 1) using 4'-bromoacetophenone as benchmark substrate. As expected, 4'-chloroacetophenone was inactive using **PdOAcNPs** (entry 5, Table 1); for 4'-iodoacetophenone, the activity was slightly lower than for the corresponding bromo-arene (entry 6 vs 1, Table 1), accordingly to a higher adsorption of iodoarenes than bromoarenes on the palladium surface;³² but in this case, the reaction was not selective, obtaining up to 40% of acetophenone. These results evidence the dramatic role of small amounts of iodides and chlorides (0.071 mol% and 0.023 mol% respectively) in the reaction medium (entries 2 and 4, Table 1), and the less severe effect of bromide (entry 3, Table 1), but also significant in comparison with **PdOAcNPs** used as catalyst (entry 3 vs 1, Table 1). It is important to note that the homo-coupling reaction was easily scaled up (entry 7 vs 1, Table 1), obtaining the same catalytic behaviour than at smaller scale.

Table 1. Preformed PdNPs as catalysts in the homo-coupling reaction of 4'-haloacetophenones.^a



entry	substrate	PdNPs	conv. (%) ^b	selectivity (4:5) ^b	yield of 4 (%) ^b
1 ^c	1	PdOAcNPs	68	9.0:1.0	61
2	1	PdClNPs	4	n.d.	n.d.
3	1	PdBrNPs	22	9.0:1.0	20
4	1	PdINPs	3	n.d.	n.d.
5	2	PdOAcNPs	<1	n.d.	n.d.
6	3	PdOAcNPs	66	6.0:4.0	41
7 ^d	1	PdOAcNPs	74	9.0:1.0	68 ^e

^a Reactions carried out under the general experimental procedure (see ESI for details). ^b Determined by GC-MS after 18 h of reaction time unless otherwise stated (tetrachloroethane was used as internal standard). ^c No reaction in the absence of catalyst. ^d Results obtained at large scale (based on 5 mmol of substrate instead of 1 mmol used under the standard conditions applied for the other entries). ^e Isolated yield.

X-fluorescence analysis of **PdOAcNPs** isolated at solid state after catalytic reaction (entry 1, Table 1), showed the presence of bromine at a relative high content, namely a Br/Pd ratio of 1/18, which represents twice the amount of bromine present in the preformed palladium nanoparticles from PdBr₂ (see

above). Consequently, the catalytic activity of **PdOAcNPs** is probably hampered due to the adsorbed bromide ions, coming from the substrate, at the metal surface, triggering a poisoning effect.

The observed reactivity trends depending on the nature of the anions present in solution correlates nicely with the Hofmeister series,³³ the known capability of ions to perturbate the hydrogen-bonded structure of bulk water,³⁴⁻³⁷ which may play a similar role to analogous 3D structured solvents by hydrogen bonding interactions such as glycerol. Namely, the Hofmeister effect for the involved anions corresponds to the following trend: $\text{CH}_3\text{COO}^- > \text{Cl}^- > \text{Br}^- > \text{I}^-$, what means that acetate anions are better solvated by glycerol than halides and in consequence they are not directly interacting with the surface. This behaviour also correlates with the better adsorption of halides, in particular iodide, at the surface.³⁸

The optimisation of the reaction conditions was carried out (temperature, base, and additives) for 4'-bromoacetophenone, being KOH (as base), hydroquinone (as reducing agent) and a catalyst loading of 1 mol% (total palladium) the optimal conditions for the synthesis of 4,4'-bisacetophenone (see Table S1 in the ESI). Under base-free conditions, the reaction did not proceed (entry 1 in Table S1). Thus, four different bases were evaluated (namely, NaOH, KOH, Na_2CO_3 , and NEt_3 ; entries 2-5 in Table S1). The results showed that strong bases such as NaOH and KOH were more efficient for the homo-coupling. In terms of reaction additives, the role of hydroquinone proved rather essential, not only to boost reaction conversion towards the homo-coupling product, but also to preclude substrate hydrodehalogenation (entry 6 vs 3 in Table S1). Hydroquinone was then tested at different amounts (from 0 to 6 equiv.),³⁹ being the optimal amount 1 equiv. (entries 3 and 7-9 in Table S1). At 120 °C, no significant changes were observed in relation to the behaviour observed at 90 °C (entries 3 and 10 in Table S1). However, a remarkable conversion decrease was observed upon recycling of the catalytic phase (entry 11 in Table S1). TEM analysis after catalysis showed the presence of different populations of nanoparticles (from *ca.* 1.5 to 14 nm; see Fig. S4 in the ESI), which can explain the loss of reactivity. This fact can be probably related to the Ostwald ripening due to palladium leaching from the nanoparticle surface promoted by halides. The presence of molecular species in the catalytic medium is most likely responsible of the hydro-dehalogenation by-product (see below, Table 2)

Concerning the use of other additives, and in particular halide salts, we realised that the addition of KI (0.2 equiv.) to the reaction medium hampered the conversion of 4'-bromoacetophenone even in the presence of base (9% conversion; see entry 1 in Table S2 in the ESI), which correlates to the experiments where using PdNPs prepared from PdI_2 (entry 4 in Table 1). This clearly demonstrates the deleterious effect of iodides for this type of Pd-based nanocatalysts, notably due to the adsorption of iodide anions at the surface, in agreement with the trend observed by Liu, Xia and co-workers in the hydrodehalogenation of halogenated aromatic compounds.³⁸ However, a recent report by Buurma *et al.* on

the enhancement of the reactivity profiles, in the presence of halide additives for the oxidative homo-coupling of boronic acids catalysed by palladium nanoparticles, suggests a leaching of palladium to the solution promoted by halides,⁴⁰ in contrast to our results.

To validate the hypothesis of the deleterious halide effect on the nanoparticle surface, we envisioned using a strong base supported on a cationic resin to withdraw halide ions from the reaction medium via ionic interaction with the polymeric beads. For this purpose, we chose the Amberlite IRA-900 hydroxide form featuring trimethyl ammonium functionalisation.⁴¹ However, the use of this cationic resin in the presence of KOH did not trigger any significant effect towards the conversion of 4'-bromoacetophenone (entry 2 in Table S2 vs entry 1 in Table 1). Moreover, the addition of NaOAc in the homo-coupling of 4'-bromoacetophenone using **PdOAcNPs** or **PdINPs** as catalyst, did not improve the reactivity, evidencing that acetate anions do not modify significantly the metal surface (entries 4 and 5 in Table S2 in the ESI).

The scope of the reaction was further studied towards the preparation of bis-aryls from moderate to good yields; for conversions lower than 15%, the homocoupling product was not isolated (Figure 2). As expected, we observed a combination of both inductive and steric effects, in particular with a preference for the substrates bearing electron-attracting and low steric-demanding groups in para position, respectively. High chemoselectivity of bis-aryl:hydrodehalogenation product (up to 9:1) was obtained for all substrates tested unless those containing a bulky group in ortho position (**15**, **16**), electron-withdrawing groups in both meta positions (**11**) or even a combination of both stereo-electronic factors led to inverse the general selectivity trends (**16**). Besides, the low conversions obtained for substrates containing nitrile groups (**9**, **14**) may be due to a plausible catalyst poisoning.

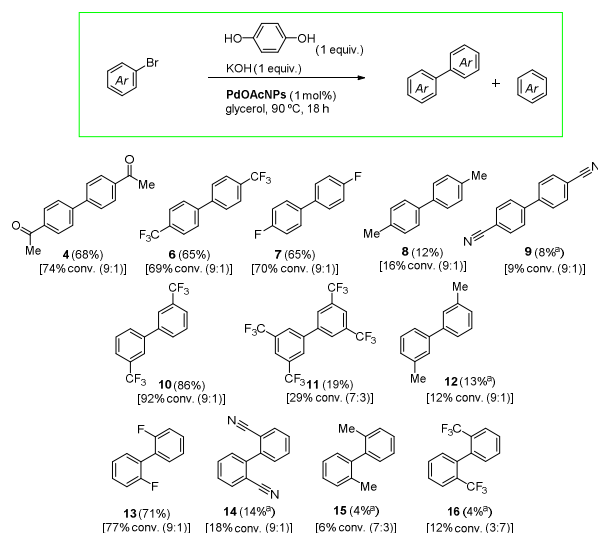


Figure 2. Reaction scope of **PdOAcNPs** catalysed homo-coupling reaction of bromoarenes. Isolated yields given in brackets; conversion and selectivity (bis-

ARTICLE

aryl:hydrodehalogenation ratio) given in square brackets (determined by GC-MS using tetrachloroethane as internal standard). ^aYield determined by GC-MS.

At this point, the need of direct comparison of nanocatalytic systems with both classical homogeneous and heterogeneous regimes described for C-C coupling reactions became mandatory. For this purpose and concerning the homogeneous catalytic system, we envisaged the use of the Herrmann-Beller palladacycle (cataCXium® C) as a source of stable Pd(II) molecular species (entries 1-2, Table 2). In toluene, the complex was inactive (entry 1, Table 2), while in glycerol, the conversion was of 62%, but favouring the formation of the hydrodehalogenation product (bis-aryl:acetophenone = 1:4). Furthermore, molecular catalytic species generated *in situ* from the corresponding metallic salts (Pd(OAc)₂, PdCl₂, PdBr₂, PdI₂) in the presence of PPh₃ were also studied (entries 3-6, Table 2). Despite PdCl₂, PdBr₂, and PdI₂ gave negligible amounts of the bis-aryl product (entries 4-6, Table 2), the use of Pd(OAc)₂ under analogous conditions gave the bis-arylation product, but in moderate yield (44%; entry 3, Table 2), due to the important formation of acetophenone (bis-aryl:acetophenone = 3:2). In the absence of PPh₃ (entries 7-9, Table 2), yields in bis-aryl were higher (entries 7-9 vs 3-5, Table 2), being Pd(OAc)₂ the most active catalytic system (Pd(CF₃COO)₂ led to a similar catalytic trend; entry 10, Table 2). Analogously to cataCXium® C, these catalysts were inactive in toluene (entries 11 and 12, Table 2). This behaviour highlights the ability of glycerol to act as a reducing agent of Pd(II) precursors towards the formation of Pd(0) species (polyol methodology synthesis of metal nanoparticles),^{42, 43} in agreement with a recent report from Kapdi and coworkers.⁴⁴ These results prompted us to further study whether the catalysts involved in such control tests had undergone any significant modifications throughout the reaction as a suspicion that some sort of palladium clusters or NPs might have formed under catalytic conditions. Thus, aliquots were taken at two different reaction times (after 15 min and 18 h of reaction) for the cataCXium® C catalytic system. Notably, the hydrodehalogenation by-product acetophenone could be detected in less than 1% by GC-MS after 15 min reaction time (conversion less than 5%), without any traces of the corresponding bis-aryl product. However, TEM analyses (carried out in glycerol solution due to the negligible vapour pressure of this solvent) of the catalytic phase just after 15 min of reaction revealed the formation of small and well-dispersed spherical nanoparticles (Figure 3).⁴⁵ These results indicate that cataCXium® C is a precursor of a palladium nanocatalyst responsible of the observed reaction outcomes. The low conversion at short times only giving acetophenone, suggests that this by-product is probably formed from molecular catalytic species. After 18 h of reaction, nanoparticles are less homogeneous in size with the formation of some aggregates, probably due to the lack of a suitable stabilising agent in the medium.

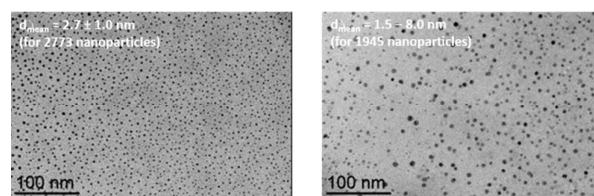
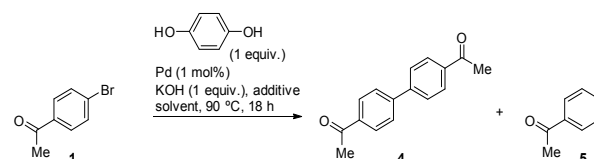


Figure 3. TEM micrographs in glycerol of cataCXium® C under catalytic reaction conditions (entry 2, Table 2): after 15 minutes (left) and 18 h of reaction (right).

For comparison purposes with a heterogeneous palladium catalyst, we used Pd/C (10 wt % metal loading on matrix activated carbon support) constituted by aggregates together with small nanoparticles ($d_{\text{mean}} = 1.7 \pm 0.4$ nm; see Fig. S5 in the ESI), in the benchmark reaction. The catalyst was highly active (>99% conversion after 18 h and 73% conversion after 6 h), but the hydrodehalogenation by-product was formed in high proportion (30%), even at shorter times (entry 13, Table 2).

Table 2. Pd-based catalytic controls in the homo-coupling reaction of 4'-bromoacetophenone.^a



entry	Pd catalyst	additive	solvent	conv. (%) ^b	selectivity (4:5) ^b	yield of 4 (%) ^b
1	cataCXium® C	-	PhMe	0	-	-
2	cataCXium® C	-	glycerol	62	2.0:8.0	12
3	Pd(OAc) ₂	PPh ₃ (2 mol%)	glycerol	75	6.0:4.0	44
4	PdCl ₂	PPh ₃ (2 mol%)	glycerol	7	5.5:4.5	4
5	PdBr ₂	PPh ₃ (2 mol%)	glycerol	5	2.0:8.0	n.d.
6	PdI ₂	PPh ₃ (2 mol%)	glycerol	<3	-	-
7	Pd(OAc) ₂	-	glycerol	94	6.0:4.0	55
8	PdCl ₂	-	glycerol	53 (71) ^c	4.5:5.5 (6.2:3.8) ^c	24 (44) ^c
9	PdBr ₂	-	glycerol	41	7.5:2.5	31
10	Pd(TFA) ₂	-	glycerol	97	5.0:5.0	48
11	PdCl ₂	-	PhMe	<3	-	-
12	Pd(OAc) ₂	-	PhMe	<3	-	-
13	Pd/C	-	glycerol	>99 (73) ^d	7.0:3.0 (7.0:3.0) ^d	70 (51) ^d

^a Reactions carried out under the general experimental procedure (see ESI for details). ^b Determined by GC-MS after 18 h of reaction time unless otherwise specified. ^c In brackets, results at 120 h. ^d In brackets, results at 6 h.

With the aim of evidencing organic intermediates in the Pd-catalysed homo-coupling process, we ran the experiments in the presence of 2,6-di-tert-butyl-4-methylphenol (BHT) as a radical trap (2 equiv.); unreacted substrate was recovered up to 98%, being the homo-coupling product and the hydrodehalogenated by-product only detected at trace levels (less

than 2%, determined by GC-MS), proving that radical intermediates are involved in the reaction pathway. In order to evidence the formation of radical species, we carried out Electronic Paramagnetic Resonance (EPR) studies for our benchmark reaction, 4'-bromoacetophenone, hydroquinone (1 equiv.) and KOH (1 equiv.) in glycerol using PdOAcNPs as catalyst (1 mol% total palladium). These studies revealed the formation of the anion radical of 4'-bromoacetophenone as reaction intermediate during the homo-coupling reaction (species I in Figure 4), together with the benzoquinone anion radical (species II in Figure 4).⁴⁶⁻⁴⁸ Thus far, 4'-bromoacetophenone radical anions could not be detected in the absence of hydroquinone (which may act as a radical stabiliser).

Thus, these results confirm the operating radical pathway for the PdNPs catalysed homo-coupling reaction in glycerol.

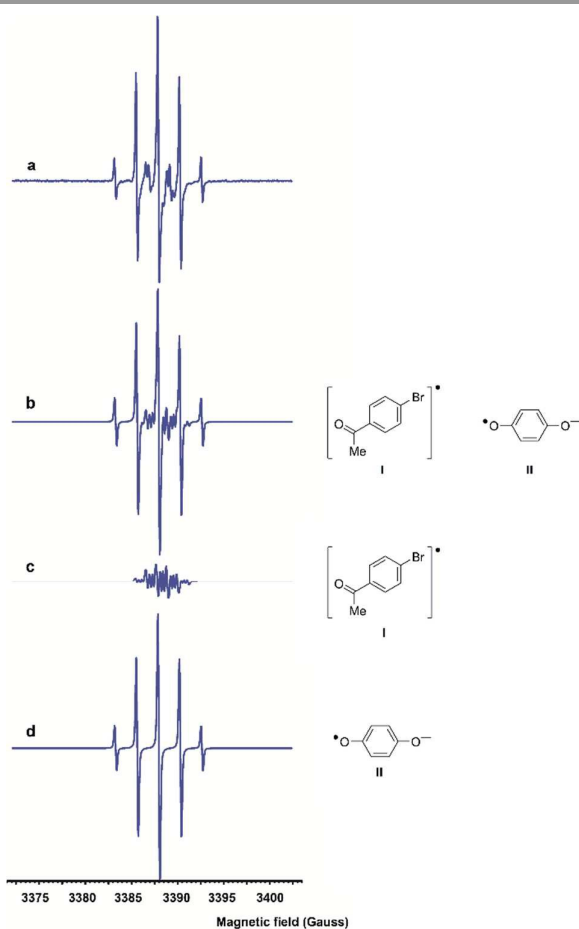
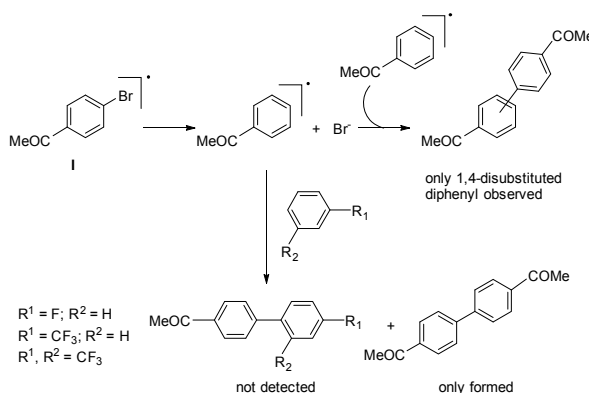


Figure 4. EPR spectra: a) Experimental EPR spectrum of the reaction sample; b) Superposition of simulated EPR spectra of both anion radical species of 4'-bromoacetophenone (I) and hydroquinone (II); c) Simulated EPR spectrum of 4'-bromoacetophenone anion radical (species I); d) Simulated EPR spectrum of hydroquinone anion radical (species II).

Despite the fact that we did not observe the acetophenone radical by EPR, we paid special attention to identify any potential coupling product that could confirm its formation *via* a base-promoted homolytic aromatic substitution mechanism.

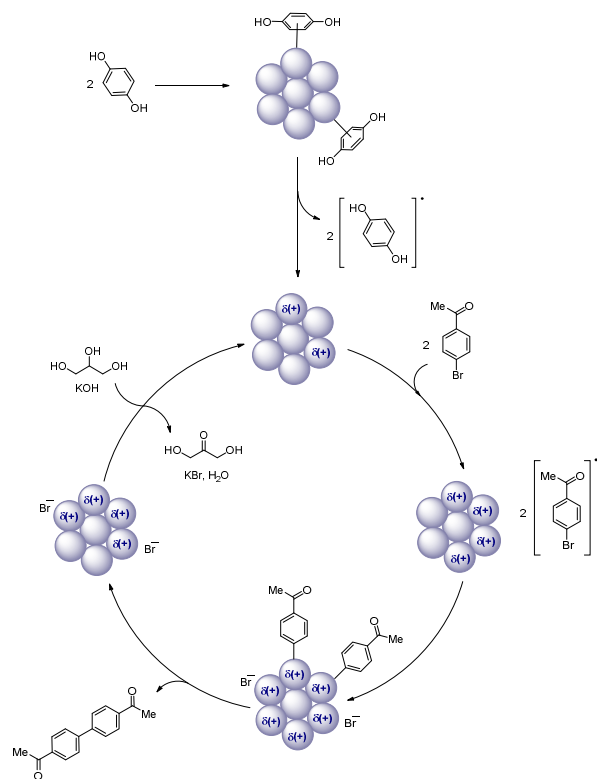
Firstly, the formation of such radical species would have led to a mixture of regioisomers; however, the product corresponding to the activation of the bromo position was exclusively obtained. Secondly, we carried out the reaction in the presence of a large excess (up to 10 equiv.) of different arenes [namely, fluorobenzene, α,α,α -trifluorotoluene, and 1,3-bis(trifluoromethyl)benzene] with the aim of trapping short-lived acetophenone radicals through formation of cross-coupling products by C-H activation (Scheme 1), but these expected products were not observed.^{49, 50} Taking into account these results, we propose that the corresponding acetophenone radicals are not formed (not detected by EPR, see Fig. S6 in the ESI), and a base-promoted homolytic aromatic substitution mechanism can be ruled out (see Fig. S7 in the ESI).



Scheme 1. Ruled out pathways for the acetophenone radical anion (species I).

The presence of such radical species could not be explained through a classical oxidative addition of bromoarenes on Pd(0) to generate a molecular Pd(II) complex that could then undergo a second oxidative addition through the formation of highly reactive Pd(IV) species. Thus, we focused on the hypothesis that the activation of bromoarenes could take place via neighbouring effects engaging different metal centres, thanks to the electronic structure of the metal nanoparticles (through the electrons at the Fermi level).

These EPR studies, together with the halide effect on the metal surface and the use of a radical trap enable us to propose a radical catalytic cycle probably involving a Pd(0)/Pd(I) manifold. These results highlight the importance of nanocatalysts to allow new reaction pathways different to those of classical homogeneous or heterogeneous catalysts. Overall, the combined experimental evidences enable us to propose a novel reaction mechanism based on an activation of aryl bromides onto the surface of the nanoparticles by intermetallic cooperative effects.



Scheme 2. Plausible reaction mechanism for the reductive homocoupling reaction mediated by Pd nanoparticles.

Conclusions

This fundamental study sheds light on how the nature of interactions at the metal surface of Pd(0) NPs plays a crucial role in determining the reactivity of catalytic systems, ultimately fostering a reaction manifold, or shutting down a reaction pathway. Notably, the discriminating role of the additives arising from the precursor salts and their impact towards gaining control of the chemoselectivity has been evidenced for catalytic transformations mediated by metallic nanoparticles in glycerol. In particular, we have identified the crucial role of counteranions on tuning the reactivity of the described catalytic systems. Thus, the presence of iodide anions serves as an effective poisoning additive to switch off the reductive homocoupling reaction manifold, probably due to both their strong interaction with the palladium surface and their low solvation by glycerol.

Herein, the importance of the surface reactivity for homo-coupling transformations could be highlighted in the present study through comparison to catalyst controls (namely Pd/C and CataCXium® C, respectively). Despite the difficulty to work under pure heterogeneous or homogenous regimes, as both leaching of molecular species in the former, or intermetallic bond formation leading to clusters and agglomeration in the latter can occur, the tailored nanoparticles prepared in this study, and PdOAcNPs in particular, provide a direct entry towards a selectivity enhancement of homo-coupling

processes in comparison to classical catalytic systems due to their defined morphology and composition, thereby impacting on the operating catalytic regimes.

In addition, we have experimentally shown that the nanocatalysed homo-coupling reaction proceeds via radical anion intermediates. By exploiting the surface reactivity of nanoparticles, it is feasible to invoke formal intermediate oxidation states, and exploit these intrinsic properties towards Pd-catalysed homo-couplings of aryl halides. For selected substrates, high conversions were achieved, furnishing the desired bis-aryl products in high yields. From a mechanistic point of view, we hypothesized that the activation of aryl halides via a surface mechanism may be achieved via neighbouring effect involving multiple metal centres, most likely through the electrons at the Fermi level. The mechanism of the coupling reaction was studied by means of radical trap and electron paramagnetic resonance (EPR) experiments, which supports a radical-based pathway. In particular, experimental evidence of the presence of aryl bromide radical anions as intermediates in the homo-coupling reaction has been provided, together with the confirmation that this transformation occurs under a radical mechanism as the homo-coupling reaction is precluded when BHT is employed as a radical scavenger.

These results highlight the importance of nanocatalysts with enhanced active surface area towards novel reaction manifolds that were otherwise limited to classical heterogeneous systems.

Conflicts of interest

There are no conflicts to declare.

Acknowledgements

The Centre National de la Recherche Scientifique (CNRS), the Université de Toulouse 3 – Paul Sabatier and Chemium SPRL are gratefully acknowledged for their financial support. The authors thank T. Girard, M. Ceresiat and L. Reginster from Chemium SPRL for fruitful discussions. The authors acknowledge C. Pradel for performing the TEM analyses, R. Lenk and E. Bellan for their help concerning the EPR studies, and N. López and M. Ortuño for mechanistic discussions.

Notes and references

1. A. Studer and D. P. Curran, *Angew. Chem., Int. Ed.*, 2011, **50**, 5018-5022.
2. A. Studer and D. P. Curran, *Nat. Chem.*, 2014, **6**, 765-773.
3. S. Zhou, G. M. Anderson, B. Mondal, E. Doni, V. Ironmonger, M. Kranz, T. Tuttle and J. A. Murphy, *Chem. Sci.*, 2014, **5**, 476-482.
4. J. A. Murphy, *J. Org. Chem.*, 2014, **79**, 3731-3746.
5. S. Zhou, E. Doni, G. M. Anderson, R. G. Kane, S. W. MacDougall, V. M. Ironmonger, T. Tuttle and J. A. Murphy, *J. Am. Chem. Soc.*, 2014, **136**, 17818-17826.

6. J. P. Barham, G. Coulthard, R. G. Kane, N. Delgado, M. P. John and J. A. Murphy, *Angew. Chem., Int. Ed.*, 2016, **55**, 4492-4496.
7. L. Zhang, H. Yang and L. Jiao, *J. Am. Chem. Soc.*, 2016, **138**, 7151-7160.
8. H. Yi, A. Jutand and A. Lei, *Chem. Commun.*, 2015, **51**, 545-548.
9. H. Yang, L. Zhang and L. Jiao, *Chem. - Eur. J.*, 2017, **23**, 65-69.
10. J. F. Bunnett, *Acc. Chem. Res.*, 1992, **25**, 2-9.
11. S. Murarka, J. Mobus, G. Erker, C. Muck-Lichtenfeld and A. Studer, *Org. Biomol. Chem.*, 2015, **13**, 2762-2767.
12. D. D. Hennings, T. Iwama and V. H. Rawal, *Org. Lett.*, 1999, **1**, 1205-1208.
13. A. Jutand and A. Mosleh, *J. Org. Chem.*, 1997, **62**, 261-274.
14. A. Monopoli, V. Calò, F. Ciminale, P. Cotugno, C. Angelici, N. Cioffi and A. Nacci, *J. Org. Chem.*, 2010, **75**, 3908-3911.
15. L. Wang, Y. Zhang, L. Liu and Y. Wang, *J. Org. Chem.*, 2006, **71**, 1284-1287.
16. V. Calò, A. Nacci, A. Monopoli and P. Cotugno, *Chem. Eur. J.*, 2009, **15**, 1272-1279.
17. A. Feiz, A. Bazgir, A. M. Balu and R. Luque, *Sci. Rep.*, 2016, **6**, 32719 (32716 pages).
18. W. Liu, X. Yang, Y. Gao and C.-J. Li, *J. Am. Chem. Soc.*, 2017, **139**, 8621-8627.
19. I. Favier, D. Madec, E. Teuma and M. Gómez, *Curr. Org. Chem.*, 2011, **15**, 3127-3174.
20. D. Pla and M. Gómez, *ACS Catal.*, 2016, **6**, 3537-3552.
21. T. Dang-Bao, D. Pla, I. Favier and M. Gómez, *Catalysts*, 2017, **7**, 207.
22. I. Favier, D. Pla and M. Gómez, *Catal. Today*, 2017, DOI: <https://doi.org/10.1016/j.cattod.2017.06.026>, DOI: [10.1016/j.cattod.2017.1006.1026](https://doi.org/10.1016/j.cattod.2017.1006.1026).
23. F. Chahdoura, C. Pradel and M. Gómez, *Adv. Synth. Catal.*, 2013, **355**, 3648-3660.
24. A. Reina, C. Pradel, E. Martin, E. Teuma and M. Gómez, *RSC Adv.*, 2016, **6**, 93205-93216.
25. S. E. Lohse, N. D. Burrows, L. Scarabelli, L. M. Liz-Marzán and C. J. Murphy, *Chem. Mater.*, 2014, **26**, 34-43.
26. N. Nalajala, A. Chakraborty, B. Bera and M. Neergat, *Nanotechnology*, 2016, **27**, 065603 (065612 pages).
27. B. T. Sneed, M. C. Golden, Y. Liu, H. K. Lee, I. Andoni, A. P. Young, G. McMahon, N. Erdman, M. Shibata, X. Y. Ling and C.-K. Tsung, *Surf. Sci.*, 2016, **648**, 307-312.
28. P. J. Hendra, *J. Chem. Soc. A*, 1967, DOI: [10.1039/J19670001298](https://doi.org/10.1039/J19670001298), 1298-1301.
29. R. A. Nyquist and R. O. Kagel, *Handbook of Infrared and Raman Spectra of Inorganic Compounds*, Academic Press, Inc, London, 1971.
30. A. Carrasquillo Jr., J.-J. Jeng, R. J. Barriga, W. F. Temesghen and M. P. Soriaga, *Inorg. Chim. Acta.*, 1997, **255**, 249-254.
31. S. S. Zinovyev, A. Perosa and P. Tundo, *J. Catal.*, 2004, **226**, 9-15.
32. M. A. Aramendía, V. Borau, I. M. García, C. Jiménez, A. Marinas, J. M. Marinas and F. J. Urbano, *C. R. Acad. Sci. II C* 2000, **3**, 465-470.
33. F. Hofmeister, *Arch. Exp. Pathol. Pharmacol.*, 1888, **25**, 1-30.
34. Claudio G. Rodrigues, Dijanah C. Machado, Annielle M. B. da Silva, Janilson J. S. Júnior and Oleg V. Krasilnikov, *Biophys. J.*, **100**, 2929-2935.
35. Z. Yang, *J. Biotechnol.*, 2009, **144**, 12-22.
36. T. López-León, M. J. Santander-Ortega, J. L. Ortega-Vinuesa and D. Bastos-González, *J. Phys. Chem. C*, 2008, **112**, 16060-16069.
37. V. Merk, C. Rehbock, F. Becker, U. Hagemann, H. Nienhaus and S. Barcikowski, *Langmuir*, 2014, **30**, 4213-4222.
38. X. Ma, S. Liu, Y. Liu, G. Gu and C. Xia, *Sci. Rep.*, 2016, **6**, 25068 (25011 pages).
39. In the absence of hydroquinone, the bis-aryl product **4** is obtained as minor product together with a relative important amount of hydrodehalogenated arene **5** (24% conversion with a selectivity of **4:5** = 3:7).
40. A. Bouleghimat, M. Othman, L. Lagrave, S. Matsuzawa, Y. Nakamura, S. Fujii and N. Buurma, *Catalysts*, 2017, **7**, 280.
41. Amberlite IRA-900 chloride form was conditioned through a column with 1 M KOH (400 mL total volume in 6 h) to trigger chloride to hydroxide exchange. The resin was then washed with deionised H₂O until no precipitate was formed in the eluates upon treatment with AgNO₃. The stationary phase was then dried under reduced pressure prior to use.
42. T.-H. Tran and T.-D. Nguyen, *Colloid. Surface B*, 2011, **88**, 1-22.
43. F. Chahdoura, I. Favier and M. Gómez, *Chem. Eur. J.*, 2014, **20**, 10884-10893.
44. V. Sable, K. Maindan, A. R. Kapdi, P. S. Shejwalkar and K. Hara, *ACS Omega*, 2017, **2**, 204-217.
45. The analogous analysis of the catalyst CataCXium after 15 min reaction time in toluene revealed the formation of Pd aggregates displaying a lesser extent of Pd NPs. The lesser extent intrinsic metal surface available is in good agreement with the lack of reactivity of this system.
46. The radical hydrodehalogenation of aryl bromides has been recently proved by Studer and co-workers using NaH and 1,4-dioxane.
47. T. Hokamp, A. Dewanji, M. Lübbesmeyer, C. Mück-Lichtenfeld, E.-U. Würthwein and A. Studer, *Angew. Chem. Int. Ed.*, 2017, **56**, 13275-13278.
48. The direct electron transfer from hydroquinone to the substrate is precluded due to its high endothermic nature (*ca.* 1.7 eV, 170 kJ/mol).
49. Fluorobenzene and α,α,α -trifluorotoluene had a slightly inhibitory effect due to biphasic nature of the reactions, but the bis-aryl homocoupling product was obtained in roughly in 25% yield (32% conversion). However, the use of 10 equiv. excess bis(trifluoromethyl)benzene hampered almost completely the reaction conversion and unreacted starting material was recovered in 94%.
50. C.-L. Sun, H. Li, D.-G. Yu, M. Yu, X. Zhou, X.-Y. Lu, K. Huang, S.-F. Zheng, B.-J. Li and Z.-J. Shi, *Nat. Chem.*, 2010, **2**, 1044-1049.